Clays and Clay Minerals, Vol. 43, No. 1, 92–104, 1995.

ZEOLITE DISTRIBUTION IN VOLCANICLASTIC DEEP-SEA SEDIMENTS FROM THE TONGA TRENCH MARGIN (SW PACIFIC)

FRÉDÉRIC VITALI, GÉRARD BLANC, AND PHILIPPE LARQUÉ

Centre de Géochimie de la Surface, CNRS UPR n°6251, Institut de Géologie Strasbourg
1 rue Blessig, 67084 Strasbourg Cédex, France

Abstract—605 m of sediments were cored in Hole 841 of the Ocean Drilling Program (ODP) at the Tonga Trench margin. The sedimentary sequence consists mainly of Miocene vitric siltstones, vitric sandstones, and volcanic conglomerates. A major consideration for selecting this site was the presence of abundant authigenic minerals (40% to 70% of the whole rock), which consist of K-feldspars, clays, thaumasite ($Ca_3Si(OH)_6CO_3SO_4$, $12H_2O$), and zeolites. The zeolite minerals include phillipsite, clinoptilolite, analcime, mordenite, chabazite, heulandite, wairakite, and erionite. The increasing amount of analcime from 257 mbsf to 470 mbsf, and the joint occurrence of mordenite and wairakite in this zone of Miocene tuffs, seems to be induced by the heat flow from a major intrusive sequence of basaltic andesite sills and dikes. This abundance of analcime in response to the thermal pulse could explain the unusual Na-depleted pore-water compositions observed in ODP Hole 841.

Key Words—Analcime, Miocene tuffs, Mordenite, Pore-water, Thermal pulse, Tonga Trench margin, Wairakite, Zeolite distribution.

INTRODUCTION

During ODP Leg 135, sediments were recovered from Hole 841 located in the forearc region of the Lau Basin (SW Pacific Ocean) (Figure 1) at a water depth of 4810 m. Hole 841 is situated on the upper trench slope, approximately 55 km west of the axis of the Tonga Trench and 60 km east of the crest of the Tonga Ridge, at 23°20.7'S, 175°17.9'W (Parson *et al* 1992). The Tonga Trench is the northern part of the Tonga-Kermadec trench system that lies between 15° and 26°S latitude, a linear distance of nearly 1200 km.

Lithologic units

The sedimentary sequence consists of 605 m of clays, vitric siltstones, volcanic conglomerate and breccias, and calcareous volcanic sandstones (Figure 2). These sediments range in age from middle Pleistocene to Pliocene. Below 605 mbsf, the hole penetrated a rhyolite volcanic complex (Parson *et al* 1992).

The sedimentary column was divided into five lithologic units. Unit I, 0–56 meters below sea floor (mbsf), is composed of clay, vitric silt, and fine ash, and ranges from middle Pleistocene to Pliocene in age. The age of Unit II (56–333 mbsf) is late Miocene. It consists of a sequence of turbidites, with a lower part composed mainly of vitric sandstone and siltstone. The clay content increases in the upper part of Unit II. This suggests an upward change from proximal to more distal deposition with an increase in water depth. The volcanic conglomerates of Unit III (333–458 mbsf), also of late Miocene age, are interpreted as proximal turbidites (Parson *et al* 1992). Units III and IV are separated by a fault breecia. The age of Unit IV (458.1–549.1 mbsf) is early middle Miocene: it is composed of volcanic siltstones, sandstones, and conglomerates. Volcanic conglomerates are found only in the lowermost part of Unit IV.

From the bottom of Unit II to the top of Unit IV, a major igneous sequence was recovered in Hole 841. This intrusive igneous sequence is a series of thin basaltic andesite units within upper Miocene volcanic siltstone and sandstone situated between 324.76 mbsf and 497.68 mbsf. The contact between the basaltic andesite and sediments includes chilled margins, hyaloclastite brecciation, and induration of the adjacent sediments. These features suggest intrusive emplacement of the igneous material into the sediments. Nine basaltic andesite units have been identified, ranging from 7 cm to almost 18 m in recovered thickness (Parson *et al* 1992). These margins show both inclined and near-horizontal dips that may constitute dykes and sills, respectively.

Beneath Unit IV there is a major unconformity, spanning approximately 13 My from the early Oligocene to the early middle Miocene. The last sedimentary unit drilled, Unit V (549.1–605 mbsf), ranges in age from late Eocene to early Oligocene. Clayey calcareous volcanic sandstone with foraminifera is the main lithology in the upper part of the Unit V. In the lowermost part of Unit V, large foraminifera bioclasts, volcanic sandstones, and calcareous volcanic sandstones with large foraminifera overlie a rhyolitic volcanic complex. The presence of this high silica, low potassium volcanic complex in the pre-Eocene stratigraphic section was unexpected.

For Hole 841, sedimentation rates were low from upper Eocene to lower Oligocene (Parson *et al* 1992).

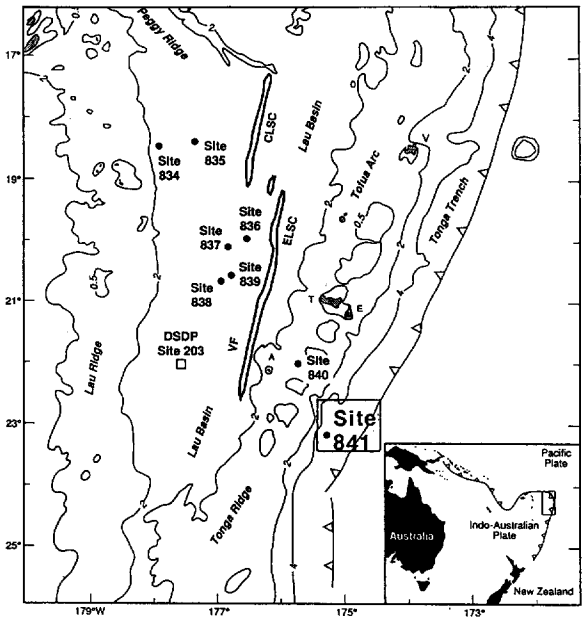

Figure 1. Regional setting of Site 841, with location of other drill sites of the Leg 135 cruise, and the major geologic features of the Tonga Trench and Lau Basin system (from Parson *et al* 1992). Islands include T = Tongatapu Island, E = 'Eua Island, V = Vavau Island, and A = Ata Island. CLSC = Central Lau Spreading Center, ELSC = Eastern Lau Spreading Center, VF = Valu Fa Ridge.

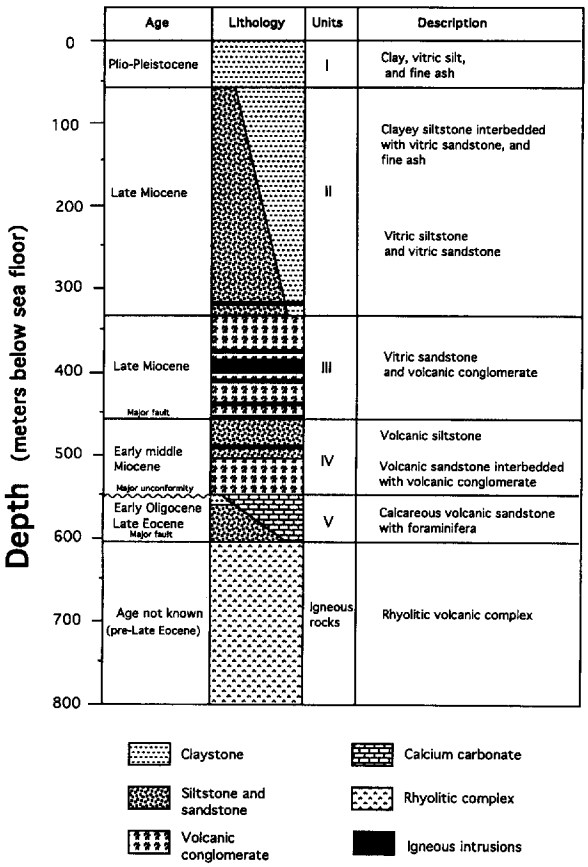

Figure 2. Schematic figure showing the distribution of the lithologic units and the igneous intrusions from Hole 841.

Sedimentation was planktonic with the occurrence of large foraminifera. With the input of volcaniclastic conglomerate and sandstone, the sedimentation rate reached 160 mm/1000 yr. Later, the sedimentation rate decreased as volcaniclastic input diminished, and finally reached 11 mm/1000 yr. during the Pliocene and Quaternary.

This drilling site provides an opportunity to determine temporal, and mineralogical variations of sediments from the Tonga Trench margin. In this paper, the origin of various and abundant zeolite minerals occurring in the sedimentary column is discussed. In addition, Hole 841 is compared with some other sites from the SW Pacific, which are rich in volcaniclastic material highly altered to secondary minerals (clays and zeolites) and which show similar patterns of interstitial water chemistry.

METHODS

Mineralogical compositions of the major mineral phases were determined on dry powdered sediments by X-Ray Diffraction (XRD) techniques using a Phillips PW 1710. The samples were run between 3° and 65° 2Θ at a scan speed of 1°/min, using CuKα radiation at 40 KV/20 mA.

Mineral percentages were estimated from peak intensities using mass absorption coefficients and chemical data (Hooton and Giorgetta 1977). Chemical analyses were performed on 73 samples from Hole 841 using a Corning Flame emission spectrometer for Na and K and an ARL 14000 arc spectrometer for the other major elements. The accuracy of our analyses was within 5% for all determined elements. Precision, as determined from duplicate analyses, was between 2% and 5%. Methods for chemical analysis are given in detail in Blanc (1994) and Vitali *et al* (1995).

Morphological features of minerals and qualitative elemental compositions were examined with a JSM 840 scanning electron microscope (SEM). Thin section microprobe analyses of zeolite minerals were made using a Cameca SX50 microprobe. For some samples, the clay fraction was separated and XRD analyses were done on oriented aggregates subjected to the following four treatments: untreated, ethylene-glycol treated, hydrazine treated, and heated (4 hours at 490°C).

RESULTS

Mineral paragenesis

The whole rock of the sedimentary column (0–605 mbsf) consists mainly of plagioclase, amorphous silica,

https://doi.org/10.1346/CCMN.1995.0430111 Published online by Cambridge University Press

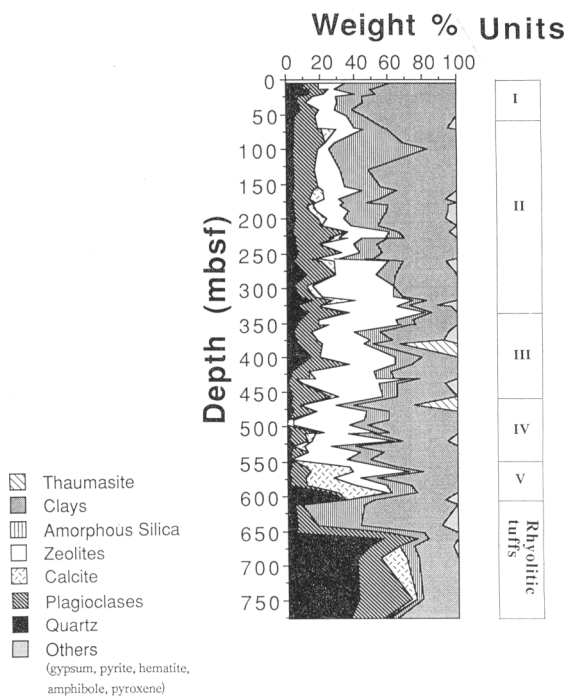

Figure 3. Mineral paragenesis with depth. Weight percent of each mineral phase was determined by XRD and chemical analysis.

clays, zeolites, and 5% to 10% quartz (Figure 3). Two samples are enriched in thaumasite, and a few others contain abundant siliceous biogenic tests (mainly radiolaria and sponge spicules). These biogenic tests are primarily localized in Unit II, which is interpreted as a sequence of turbidites (Parson *et al* 1992). The amount of carbonate in Hole 841 is very low (between 0% and 5%), with the exception of Unit V, which consists of calcareous volcanic sandstones with foraminifera. The calculated concentration of halite is an artefact due to the evaporation of seawater during preparation of dry powdered samples. Thus, on Figure 3, the weight percent of the others mineral phases was normalized to 100% on a halite-free basis.

The youngest unit of the rhyolitic volcanic complex is composed mainly of quartz (30% on average) and plagioclase (20% on average). Alteration is very important in this rhyolitic tuff Unit, with the formation of secondary calcite and various types of clays.

Secondary silicate minerals

The secondary minerals of Hole 841 consist of K-feldspars, clays, thaumasite, and zeolites. The amount of K-feldspar was too low to be detected by X-ray diffraction, however, rare occurrences of this mineral were observed with the SEM (Plate 1A). K-feldspar has been observed in 296.4 mbsf (Core 135 841B 15R1), with chlorite growing on it, and at 557.4 mbsf (Core 135 841B 42R3).

Preliminary results from analyses made on 27 samples (Table 1) of Hole 841 show that interlayered illite/smectite is the most important clay mineral in these sediments. On the basis of XRD patterns of the clay fraction, smectite content of the interlayered illite/smectite exceeds 70% in most of samples from the units IV and V. Perfect XRD of smectite are found only in sediments from 296.4 to 410 mbsf. In this interval of vitric sandstone of late Miocene age containing igneous intrusions, corrensite, which was defined as a 1:1 regular interstratification of trioctahedral chlorite with trioctahedral smectite (Bailey 1982), and chlorite (Plate 1B) constitute the other major clay phases (Vitali *et al*, in preparation). The stability field of corrensite was previously estimated between 200 and 300°C (Desprairies and Jehanno 1983). Corrensite occurs only in this interval, whereas chlorite exists in the other parts of the sedimentary column but as a minor phase (less than 10% of the clay fraction).

In the rhyolitic tuffs Unit, close to the major fault separating this unit to the deepest sedimentary unit, the rhyolitic volcanic complex is extremely altered to interlayered illite/smectite, chlorite, and illite. Below 700 mbsf, the interlayered illite/smectite disappears and the clay fraction consists of chlorite, illite, and kaolinite.

Another secondary mineral present in the Hole 841 is a ($Ca_3Si(OH)_6CO_3SO_4$, $12H_2O$) mineral called thaumasite. The occurrence of thaumasite in Miocene tuff is rare. The first description of thaumasite associated with zeolites in deep sea sediments was made during Leg 129 ODP in the Mariana basin (Karpoff *et al* 1992). In Hole 841, thaumasite occurs as a major component in the following two samples of Miocene sediments: at 380.78 mbsf (Core 135 841B 24R1) in volcanic breccia, and at 470.27 mbsf (Core 135 841B 33R2) in volcanic siltstone. This mineral has an upper thermal stability limit of 60 ± 5°C (Giampaolo 1986). At higher temperatures, thaumasite decomposes to calcite and gypsum. Thaumasite of Hole 841 was described by Schöps and Herzig (1994) at 325.14 mbsf (Core 135 841B 18R2), filling a 0.5 cm fissure in basaltic andesite, and at 530.30 mbsf (Core 135 841B 39RCC) as a component of Miocene volcaniclastic sediment.

Zeolites constitute the major authigenic minerals occurring at Hole 841. These minerals occur across the entire sedimentary sequence, showing no variations in XRD peak width with depth. Zeolite minerals represent 10 wt. % to 20 wt. % of the sedimentary column between 0 and 260 mbsf. The proportion of zeolites roughly increases from 260 mbsf to the rhyolitic tuffs Unit (between 20 wt. % and 45 wt. % of the whole rock). The formation of zeolite species depends mainly upon the nature of the Al-Si alumino-silicate source (% of glass with respect to crystalline material), chem-

Table 1. Variety of clays from Site 841 based on XRD analysis and expressed in relative weight percent of each clay species into the clay fraction: E < 5%, 5% < X < 30%, 30% < XX < 70%, XXX > 70%.

Units	No. ODP	Depth (mbsf)	Illite	I/S	I/S (S > 70%)	Smectite	Corrensite	Chlorite	Kaolinite
II	841B 4R1 (97–98)	190.08		XXX				X	
	841B 10R1 (130–132)	248.37	X	XXX				X	E
	841B 13R4 (46–48)	280.57			XXX			E	
	841B 15R1 (135–150)	296.4				XXX		X	
	841B 17R3 (57–59)	317.38					XX	XX	
III	841B 24R1 (7–9)	380.78					XX	XX	
	841B 27R1 (42–44)	410.13				XXX	X		
	841B 29R1 (130–150)	430.6				XXX		E	
IV	841B 32R1 (48–50)	458.59			XXX				
	841B 34R1 (137–140)	478.89		XXX				E	
	841B 35R3 (42–44)	490.53		XXX					
	841B 36R2 (53–57)	498.85		XXX					
	841B 37R3 (0–13)	509.5			XXX				
	841B 37R4 (7–9)	510.98			XXX			E	
	841B 38R3 (115–118)	520.27			XXX				
	841B 39R2 (41–43)	527.62			XXX				
	841B 40R2 (8–20)	537	E		XXX			X	E
	841B 41R2 (104–107)	547.56			XXX				E
V	841B 42R3 (0–9)	557.4				XXX			
	841B 43R1 (95–97)	564.96				XXX		E	E
	841B 44R1 (52–54)	574.13				XXX			
Rhyolitic tuffs	841B 47R2 (120–122)	605.31	XX	X				XX	
	841B 48R1 (37–39)	612.68			XXX				
	841B 51R2 (0–10)	642.8			XXX			E	
	841B 54R2 (76–79)	672.47	E			XXX		X	
	841B 62R1 (130–150)	748.7	X					XX	XX
	841B 65RC (20–22)	776.2	XX					XX	

istry of the pore fluid, temperature, and time (Hay 1966, 1986). The zeolite minerals identified in Hole 841 include phillipsite, analcime, clinoptilolite, mordenite, chabazite, heulandite, wairakite, erionite, and traces of merlinoite and harmotome. Analcime, clinoptilolite, and phillipsite are common components of deep sea sediments, whereas the other zeolite minerals present in Hole 841 are not commonly found in deep sea sediments (Stonecipher 1976). However, most of these zeolites have recently been described by Marsaglia and Tazaki (1992) in Hole 793 sandstones from the Izu-Bonin Forearc (Taylor *et al* 1990).

Zeolite distribution

Phillipsite and analcime are the two most common zeolites of Hole 841 (Table 2). Phillipsite is a frequent component of Pacific deep sea sediments and also of the vitric tuff which was zeolitized under near surface conditions (Gottardi and Galli 1985). It is abundant in Miocene or younger sediment (Stonecipher 1976, Boles and Wise 1978, Kastner and Stonecipher 1978). Phillipsite is the main zeolite present in the upper part of the Hole 841 and appears as tiny rods (about 1 μm wide and 10 μm long). This mineral predominates in Units I and II (late Miocene to Pleistocene), and in the calcareous unit V (late Eocene–early Oligocene). Another potassic zeolite, merlinoite (Passaglia *et al* 1977), has been detected at 171.3 mbsf (Core 135 841B 2R1) in clayey siltstone interbedded with coarse vitric sandstone (late Miocene).

Analcime is detected mainly between 260 and 550 mbsf and is the most important zeolite of the sedimentary column (Plate 1C), with a size predominantly in the 20–63 μm fraction. This analcime is associated with other zeolites (phillipsite, mordenite, wairakite, clinoptilolite, heulandite, chabazite, and clays, as observed by X-Ray diffraction and SEM (Plate 1D). Most often, analcime appears as well-formed crystal in geodes, sometimes with mordenite, which occurs at Hole 841 as compact bundles of needle like particles, mostly less than 1 μm across and 8–10 μm long (Plate 2A), or as isolated rods growing on analcime crystals (Plates 2B and 2C). However, in the upper limit of the analcime zone, analcime was also detected (sample 841B 15R1, 296.4 mbsf) filling the center of few veinlets approximately 100 μm wide; mordenite occupied the rim of the veinlet (Plate 2D).

Wairakite, the zeolite corresponding to the calcic pole of the analcime-wairakite solid-solution series, was clearly identified at 345.42 mbsf (Core 135 841B 20R2), and at 400.26 mbsf (Core 135 841B 26R1).

Although clinoptilolite is particularly common in deep sea sediments (Stonecipher 1976, Kastner and

https://doi.org/10.1346/CCMN.1995.0430111 Published online by Cambridge University Press

Table 2. Zeolite distribution in Site 841 based on XRD analysis and expressed in relative weight percent of each zeolite species into the zeolitic fraction: E < 5%, 5% < X < 25%, 25% < XX < 35%, 35% < XXX < 60%, XXXX > 60%.

Age	Units	No. ODP	Depth (mbsf)	Phillip-site	Clinoptilolite	Analcime	Erionite	Chabazite	Heulandite	Mordenite	Others
Plio-Pleistocene	I	1H-4 (140–150)	6	X							
		2H-3 (80–82)	13.81	E		E					
		2H-4 (140–150)	14.5	E							
		3H-2 (90–92)	20.4	X		E					
		3H-4 (140–150)	24	X							
		4H-4 (140–150)	33.5	X		E					
		5H-3 (89–91)	43.9	E							
		6H-4 (140–150)	52.5	X							
Late Miocene	II	8H-3 (140–150)	70	X							
		9X-1 (67–69)	72.38	X		E					
		11X-1 (44–46)	91.45	E							
		12X-CC (2–4)	100.75	E							
		15X-1 (56–57)	130.17	X							
		18X-1 (13–15)	154.04	X							
		19X-1 (52–55)	159.64	X							
		2R1 (142–150)	171.3	E							Merlinoite E
		21X-1 (30–32)	177.21	X							
		3R2 (35–38)	181.27	X	E						
		4R1 (97–98)	190.08	X		X					
		5R1 (142–150)	200.2	E							
		6R1 (137–138)	209.78	X							
		7R1 (50–51)	218.61	X							
		8R1 (40–42)	228.11	X		E					
		8R1A (75–85)	228.5								
		9R1 (7–8)	237.48	X							
		10R1 (130–132)	248.31	X							
		11R1 (61–74)	257.4				X				
		11R2 (65–67)	257.54	X							
		12R1 (84–86)	261.15			E	X				
		13R4 (46–48)	280.57		X	X					
		15R1 (135–150)	296.4		X	XX			E		
		16R5 (102–104)	311.63		E	XX				E	
		17R3 (57–59)	317.38	E		XX					
		18R1 (131–133)	324.82	E		XX					
		18R2 (77–95)	325.9			XXX					
Late Miocene	III	19R1 (99–101)	334.2			XXX					
		20R2 (141–143)	345.42			XXX					Wairakite E
		21R1 (12–32)	352.4			XXX	E			X	
		21R1A (113–116)	353.25			XXX				E	
		22R2 (15–17)	363.06			XX					
		23R3 (62–66)	374.75			XX					
		24R1 (7–9)	380.78			XX					
		26R1 (15–17)	400.26			XX					Wairakite X
		27R1 (42–44)	410.13			X					
		28R1 (130–131)	420.71	E		XX				X	
		29R1 (130–150)	430.6			XX				X	
		29R2 (12–14)	430.75			XXXX					
		30R1 (20–23)	439.02			XXX					
Early middle Miocene	IV	32R1 (48–50)	458.59			X		X			
		33R2 (96–98)	470.27			XX					
		34R1 (137–140)	478.89	X	X						
		35R3 (42–44)	490.53	X				XX			
		36R2 (53–57)	498.85				X	X	X		
		37R3 (0–13)	509.5				X	X	X		
		37R4 (7–9)	510.98		X			X	X		
		38R3 (115–118)	520.27			XX		X			
		39R2 (41–43)	527.62				X				
		40R2 (8–20)	537		X	E	X		X		
		41R2 (104–107)	547.56	E		XX					

https://doi.org/10.1346/CCMN.1995.0430111 Published online by Cambridge University Press

Table 2. Continued.

Age	Units	No. ODP	Depth (mbsf)	Phillip-site	Clinoptilolite	Analcime	Erionite	Chabazite	Heulandite	Mordenite	Others
E. Oligocene L. Eocene	V	42R3 (0–9)	557.4	X							Harmotome E
		43R1 (95–97)	564.96	XX							
		44R1 (52–54)	574.13	X							
		45R1 (53–55)	583.84	X							
		46R2 (50–52)	594.91	E							
Age not known	Rhyolitic Tuffs Unit	47R2 (120–122)	605.31								
		48R1 (37–39)	612.68								
		51R2 (0–10)	642.8								
		52R2 (35–37)	652.76								
		53R1 (130–150)	662.1								
		54R2 (76–79)	672.47								
		56R1 (28–31)	689.7								
		62R1 (130–150)	748.7								
		65 RCC (103–150)	776.2			E					

Stonecipher 1978), its presence was only reported in a few samples from Hole 841, where it appears as abundant well formed tabular crystals, approximately 5 μm in size (Plate 3A), often associated with analcime and clays (Plate 3B). Clinoptilolite occurs in Unit II of late Miocene age and in Unit IV of early middle Miocene age.

The other zeolites present in the Hole 841 are a solid solution with clinoptilolite called heulandite (Boles 1972, Gottardi and Galli 1985) and chabazite. Their occurrences are virtually restricted to the Unit IV. This unit of volcanic siltstone and volcanic sandstone interbedded with volcanic conglomerate contains the greatest variety of zeolites in Hole 841.

Zeolite chemistry

Microprobe analyses have been made on the predominant zeolite mineral, i.e., analcime, and on a Na-Ca mordenite, closely associated with analcime in Hole 841. The chemical formula of each analysis of analcime and mordenite was recalculated on the basis of 96 oxygens (Passaglia 1975, Gottardi and Galli 1985) and the balance error:

$$E = \frac{Al(+Fe^{3+}) - Al_{theor.}}{Al_{theor.}} \times 100$$

of each analysis was calculated (Tables 3a and 3b). $Al(+Fe^{3+})$ corresponds to the atomic coefficient of Al plus the coefficient of Fe^{3+} given by the analysis and $Al_{theor.} = Na + K + 2(Ca + Mg + Sr + Ba)$. A positive error shows an excess of trivalent cation, whereas a negative error an excess of exchangeable cations (Passaglia 1970). In Hole 841, Sr and Ba whole rock concentrations are less than 0.01% and could be neglected. A value of 0 for the balance error fits with a perfect analysis. In any case, only analyses with a low E (< 10%) should be considered acceptable (Passaglia and Vezzalini 1985, Gottardi and Galli 1985). 71% of analyses made on selected samples from Hole 841 met this criterion. This corresponds to 35 analcime and 4 mordenite minerals from 3 representative samples of the analcime zone (841B-15R1, 296.4 mbsf; 841B-21R1, 352.4 mbsf, and 841B-29R1, 430.6 mbsf). The chemical analysis and structural formula are reported in Tables 3a and 3b, respectively.

Analcime and associated mordenite vary only very slightly in their chemical composition (Tables 3a and 3b). Analcime from Hole 841 has a composition close to the stochiometric formula from Gottardi and Galli (1985), with, however a slight enrichment in Si associated with a slight deficiency in Al and Na (Figure 4a). The atomic coefficients of Si, Al, Na and Ca average 33.5, 14.5, 14.5 and 0.1, respectively, using samples with the lowest deviation error. The 0.8–1.5 wt. % CaO measurements of few samples (21R1 AP4 and 29R1 EP51 previously) (Table 3b and 3c, Figure 4b) probably result from a contamination of the analysis by the rods of associated mordenite.

The atomic proportions of Si and Al in the mordenite range from 37.44 to 40.04 and 7.76 to 10.12 atomic percent, respectively (Table 3d). This fit well with the values obtained in the detailed study made on this mineral by Passaglia (1975). The slight variation of mordenite composition concerns mainly the extra-framework cation (Figure 4b). The K and Mg content is low in all samples studied, the Ca-atomic coefficients range in the interval 1.6–2.5 previously given in Gottardi and Galli (1985), whereas the Na-atomic coefficients range between 5.03 (sample 29R1 DP25) and 5.92 (sample 15R1 ME4), which is invariably slightly higher than the interval 2–5 given by the same authors. Thus in Hole 841, this mineral could be considered a Na-mordenite.

https://doi.org/10.1346/CCMN.1995.0430111 Published online by Cambridge University Press

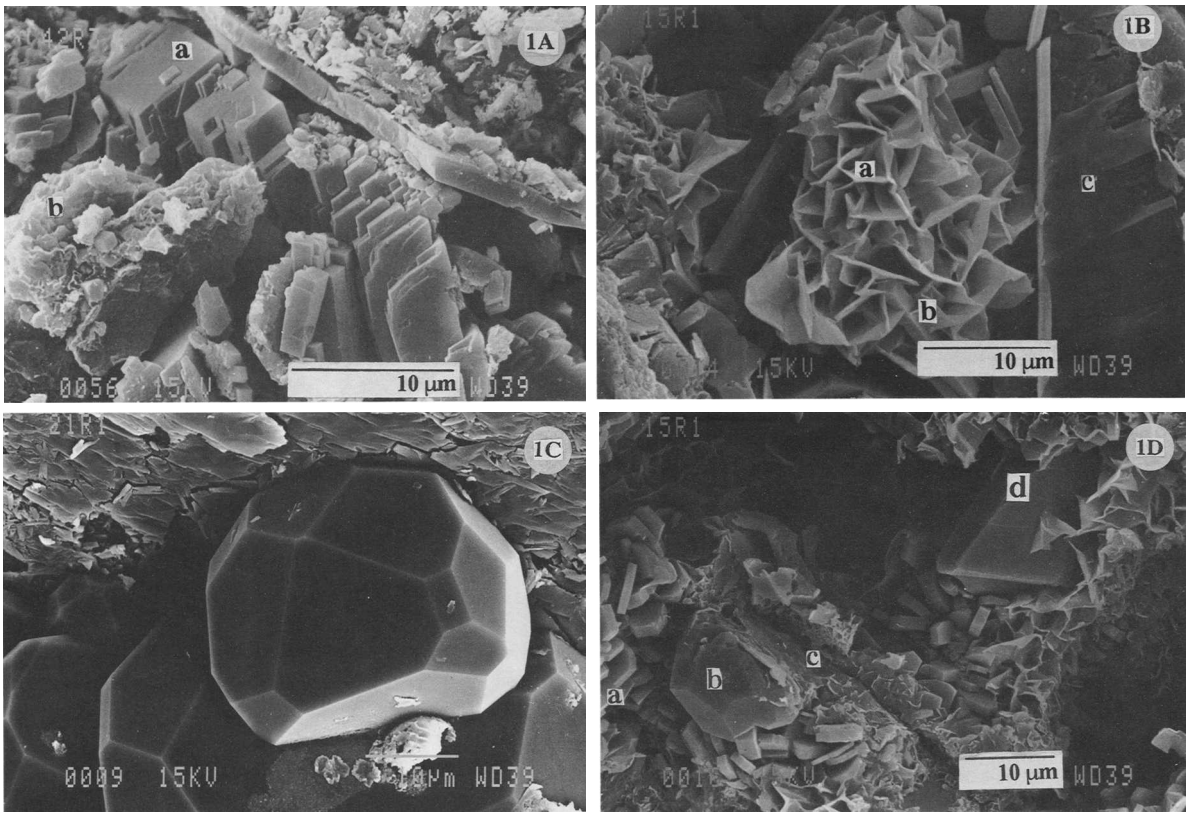

Plate 1A. (a) Authigenic K-Feldspar, and (b) smectite (Core 135 841B 42R3; 557.4 mbsf).

Plate 1B. (a) Chlorite layers with (b) zeolite rods, and (c) authigenic K-Feldspar (Core 135 841B 15R1; 296.4 mbsf).

Plate 1C. Euhedral analcime crystals from Core 135 841B 21R1 (352.4 mbsf).

Plate 1D. (a) Clinoptilolite, (b) subsequent analcime growing on it, (c) smectite, and (d) a K-feldspar with (e) layers of chlorite (Core 135 841B 15R1; 296.4 mbsf).

DISCUSSION

Effects of a thermal pulse

The results presented in this paper show a zeolite distribution that can be summarized from the top to the bottom of the sedimentary column by the sequence:

phillipsite
clinoptilolite + analcime
analcime (alone or occasionally with either wairakite or mordenite)
analcime, phillipsite, clinoptilolite, erionite, chabazite, heulandite
phillipsite

Such zeolite zonation may be attributed to the superposition of two distinct phenomena: At first, a simple burial diagenesis with formation of phillipsite and clinoptilolite, depending on depth and types of sediments encountered, and secondly, a "baking" of one part of the sedimentary column. This last effect reflects the heat flow caused by the intrusion of the major igneous sequence between 324.76 mbsf and 497.68 mbsf.

Analcime is the most abundant zeolite mineral in this "baked" part of the sedimentary column. Just above the zone of basaltic andesite dykes and sills, analcime is associated with clinoptilolite (Plate 1D). SEM studies suggest that analcime crystallized after clinoptilolite (Plates 1D and 3B). In the sedimentary column of Hole 841, the upper boundary of the analcime zone was recognized around 315 mbsf.

The measured thermal gradient of the sedimentary column during the cruise was 28.4°C/km (Parson *et al* 1992). Thus, whereas clinoptilolite was probably generated at least in part by burial diagenesis, following the reaction

$$\text{phillipsite} + H_4SiO_4 \rightarrow \text{clinoptilolite} + H_2O$$

(Couture 1977, Boles and Wise 1978)

and the crystallization of analcime is probably related to the heat flow resulting from the cooling of the igneous intrusion according to the reaction:

https://doi.org/10.1346/CCMN.1995.0430111 Published online by Cambridge University Press

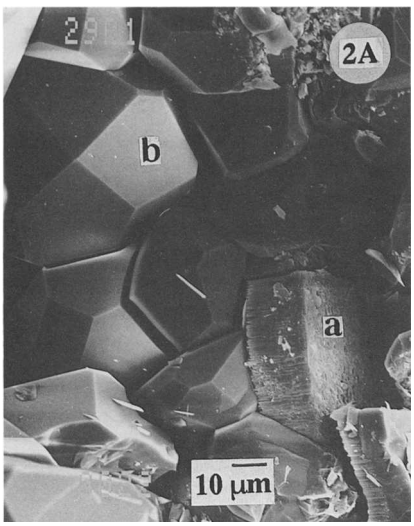

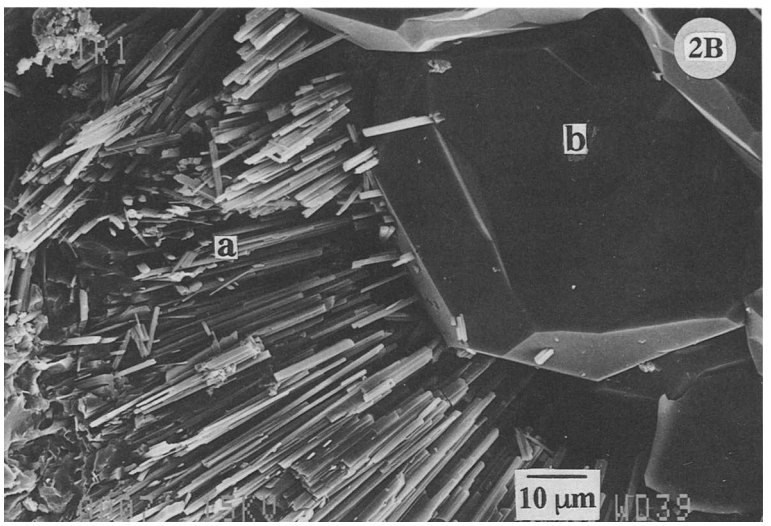

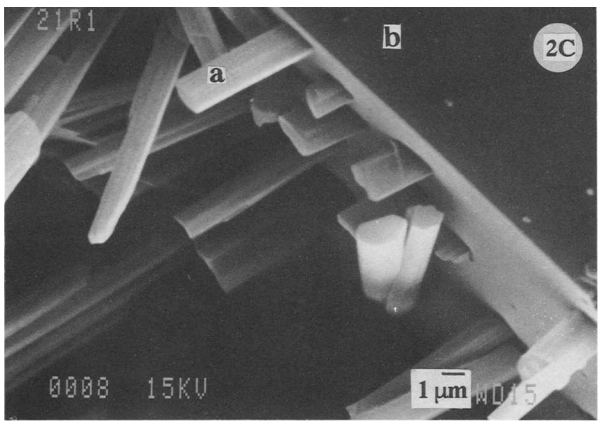

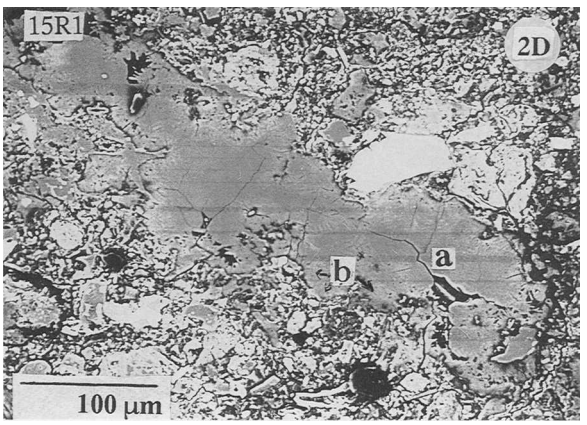

Plate 2A. (a) Compact bundle of mordenite in (b) a geode of analcime (Core 135 841B 29R1; 430.6 mbsf).

Plates 2B and 2C. (a) Rods of mordenite associated to (b) an analcime crystal (Core 135 841B 21R1, 352.4 mbsf).

Plate 2D. Veinlet of zeolites in volcaniclastic sediments of Hole 841 (thin section from Core 135 841B 15R1; 296.4 mbsf). (a) Analcime fills the center of the veinlet whereas mordenite occupies the rim.

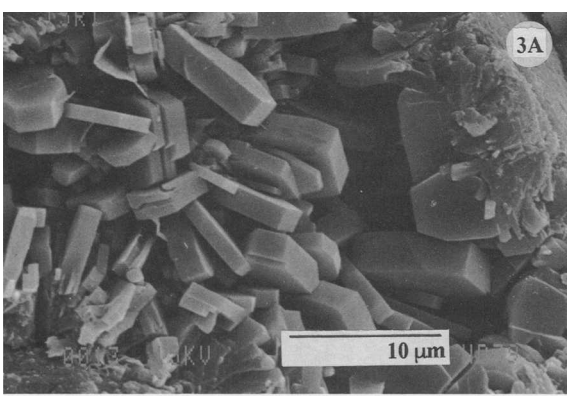

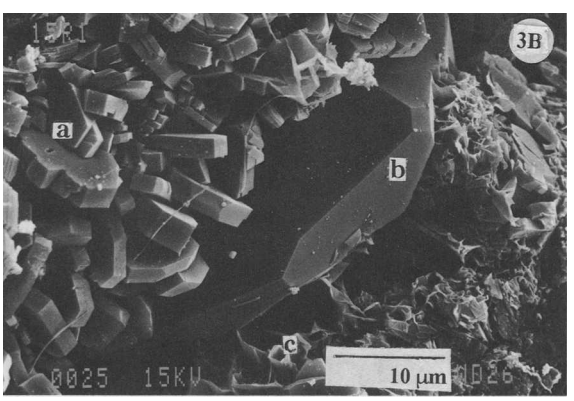

Plate 3A. Assemblage of euhedral tabular-form clinoptilolite (Core 135 841B 15R1; 296.4 mbsf).

Plate 3B. Growth of analcime crystal from clinoptilolite with corroded aspect, and presence of chlorite sheets on both zeolitic minerals, as a reequilibrium phase (Core 135 841B 15R1; 296.4 mbsf).

https://doi.org/10.1346/CCMN.1995.0430111 Published online by Cambridge University Press

clinoptilolite + Na → analcime + SiO_2 + K + Ca + Mg + H_2O

Several studies have indicated that relatively elevated temperature favors mordenite formation (e.g., Sheppard *et al* 1988, Barth-Wirsching and Höller 1989), but temperatures lower than 280°C are required for a Na-mordenite (Nakajima and Ueda 1990). The upper stability limit for analcime is higher, around 300–320°C (Liou 1971, Kristmannsdöttir and Tomasson 1978, Kusakabe *et al* 1981, Nakajima and Ueda 1990).

The crystallization of mordenite from Hole 841 seems to represent formation of a reequilibrium phase, visible in few samples. Mordenite crystallization could have 2 origins:

Table 3a. Microprobe analyses (weight %) and structural formula (atomic coefficient) of analcime calculated on the basis of 96 oxygens, Core 135 841B 15R1; 296.4 mbsf.

	15R1 AP55	15R1 AP56	15R1 FP57	15R1 BP58	15R1 ME1	15R1 ME3
SiO_2	61.8	61.71	62.36	64.86	58.63	58.66
Al_2O_3	24.00	23.77	23.12	21.74	25.35	25.24
MgO	0.00	0.01	0.00	0.01	0.00	0.00
CaO	0.00	0.02	0.08	0.92	0.1	0.00
Na_2O	14.04	14.3	14.33	12.3	15.8	15.87
K_2O	0.03	0.00	0.02	0.17	0.00	0.00
Fe_2O_3	0.13	0.19	0.1	0.00	0.12	0.23
Si	32.99	32.99	33.32	34.37	31.69	31.71
Al	15.1	14.98	14.56	13.57	16.15	16.08
Mg	0.00	0.01	0.00	0.01	0.00	0.00
Ca	0.00	0.01	0.04	0.52	0.06	0.00
Na	14.53	14.82	14.84	12.63	16.56	16.63
K	0.02	0.00	0.01	0.11	0.00	0.00
Fe	0.05	0.07	0.04	0.00	0.05	0.09
E %	4.15	1.25	−2.33	−1.7	−2.85	−2.71

—the direct alteration of the abundant volcaniclastic sediments

—alteration of analcime minerals, following the reaction:

analcime + SiO_2 + K + Ca + Mg + H_2O → mordenite + Al + Na

In addition, the occurrence of wairakite suggests high temperatures in the sedimentary column (Liou 1971, Seki 1973, Surdam 1973, Boles 1977). Experimental studies on zeolite equilibria indicate that temperatures of alteration may have been in excess of 200°C for the formation of wairakite (Barth-Wirsching and Höller 1989, Liou *et al* 1991); the measured upper stability limit of this zeolite is 400°C (Liou 1971, Nakajima and Ueda 1990). Present day zeolitic hydrothermal alteration is known in many parts of the world, including Wairakei in New Zealand (Steiner 1955), the Onikobe geothermal field in Japan (Seki *et al* 1969), in Iceland (Kristmannsdöttir and Tomasson 1978), and Yellowstone National Park in USA (Bargar *et al* 1981). In Iceland, wairakite is present only in volcanic zones with temperatures close to 250°C and is associated with analcime. We can rank the upper limit of temperature stability for the zeolites as follows: mordenite < analcime < wairakite.

Zeolite, known to be low pressure minerals (P < 3.5 Kb.) (Liou 1971, Nakajima and Ueda 1990), has grown in Hole 841 at pressures lower than 1 Kb. Thus, other factors seem to be more important than pressure in controlling the secondary mineral paragenesis in the Miocene volcanic sandstone and conglomerate of Hole 841. They appear to be temperature and the composition of the fluid brought into the sedimentary column during the intrusions. Thus, in Hole 841 the zone with analcime + (mordenite or wairakite), and also the in-

Table 3b. Microprobe analyses (weight %) and structural formula (atomic coefficient) of analcime calculated on the basis of 96 oxygens, Core 135 841B 21R1; 352.4 mbsf.

	21R1 AP1	21R1 AP2	21R1 AP4	21R1 AP5	21R1 BP8	21R1 BP9	21R1 CP12	21R1 CP13	21R1 CP14	21R1 HP17	21R1 HP19	21R1 GP20
SiO_2	62.45	62.72	70.19	63.31	63.55	64.00	63.47	63.14	62.71	63.01	66.34	63.97
Al_2O_3	23.42	23.1	18.95	22.91	22.79	22.65	23.15	22.98	22.91	22.84	20.99	22.89
MgO	0.00	0.04	0.00	0.00	0.00	0.00	0.01	0.01	0.02	0.03	0.00	0.01
CaO	0.00	0.06	1.33	0.18	0.28	0.12	0.09	0.04	0.08	0.09	0.81	0.14
Na_2O	14.06	13.94	9.36	13.61	13.18	13.07	13.1	13.7	14.08	13.82	11.59	12.93
K_2O	0.07	0.08	0.09	0.00	0.06	0.03	0.07	0.00	0.01	0.03	0.05	0.07
Fe_2O_3	0.00	0.07	0.07	0.00	0.15	0.12	0.12	0.13	0.19	0.18	0.22	0.00
Si	33.31	33.44	36.52	33.67	33.77	33.94	33.69	33.6	33.46	33.58	34.96	33.9
Al	14.72	14.52	11.62	14.36	14.27	14.16	14.48	14.41	14.41	14.34	13.04	14.3
Mg	0.00	0.04	0.00	0.00	0.00	0.00	0.01	0.01	0.02	0.03	0.00	0.01
Ca	0.00	0.03	0.74	0.1	0.16	0.07	0.05	0.02	0.04	0.05	0.46	0.08
Na	14.54	14.41	9.45	14.03	13.57	13.44	13.48	14.13	14.57	14.28	11.84	13.29
K	0.04	0.05	0.06	0.00	0.04	0.02	0.04	0.00	0.01	0.02	0.04	0.05
Fe	0.00	0.03	0.02	0.00	0.06	0.05	0.05	0.05	0.08	0.07	0.09	0.00
E %	0.94	−0.39	5.93	0.92	2.87	4.45	6.54	1.87	−1.46	−0.31	2.59	5.82

https://doi.org/10.1346/CCMN.1995.0430111 Published online by Cambridge University Press

Table 3c. Microprobe analyses (weight %) and structural formula (atomic coefficient) of analcime calculated on the basis of 96 oxygens, Core 135 841B 29R1; 430.6 mbsf.

	29R1 AP24	29R1 DP26	29R1 DP27	29R1 DP28	29R1 EP30	29R1 EP31	29R1 HP34	29R1 IP39	29R1 EP46	29R1 EP47	29R1 EP48	29R1 EP49	29R1 EP50	29R1 EP51	29R1 EP52	29R1 CP53	29R1 CP54
SiO_2	62.82	69.01	63.55	65.98	68.43	67.82	62.73	64.9	63.18	65.24	68.57	65.73	62.89	70.22	62.87	64.96	62.32
Al_2O_3	22.87	19.16	22.62	20.95	19.8	20.17	23.21	21.63	22.56	21.39	19.69	20.89	22.39	18.64	22.53	21.78	23.74
MgO	0.03	0.01	0.02	0.00	0.00	0.00	0.02	0.00	0.01	0.01	0.02	0.00	0.00	0.01	0.02	0.00	0.00
CaO	0.00	0.94	0.11	0.61	0.87	0.69	0.01	0.23	0.15	0.41	0.88	0.35	0.14	1.08	0.12	0.3	0.00
Na_2O	13.99	10.82	13.63	12.46	10.87	11.21	13.98	13.24	13.79	12.89	10.8	12.88	14.32	9.63	14.46	12.79	13.91
K_2O	0.03	0.06	0.07	0.00	0.00	0.08	0.04	0.00	0.06	0.03	0.01	0.02	0.00	0.01	0.00	0.01	0.00
Fe_2O_3	0.26	0.00	0.00	0.00	0.03	0.02	0.00	0.00	0.25	0.02	0.03	0.12	0.27	0.41	0.00	0.16	0.03
Si	33.5	36.11	33.8	34.86	35.82	35.58	33.43	34.4	33.67	34.55	35.89	34.78	33.6	36.56	33.58	34.39	33.21
Al	14.38	11.82	14.18	13.04	12.22	12.47	14.58	13.51	14.17	13.35	12.14	13.03	14.1	11.44	14.18	13.59	14.91
Mg	0.03	0.01	0.02	0.00	0.00	0.00	0.02	0.00	0.01	0.01	0.02	0.00	0.00	0.01	0.02	0.00	0.00
Ca	0.00	0.53	0.06	0.34	0.49	0.39	0.01	0.13	0.09	0.24	0.49	0.2	0.08	0.6	0.07	0.17	0.00
Na	14.47	10.98	14.06	12.76	11.04	11.4	14.44	13.61	14.25	13.23	10.96	13.22	14.83	9.72	14.97	13.13	14.37
K	0.02	0.04	0.05	0.00	0.00	0.05	0.03	0.00	0.04	0.02	0.01	0.02	0.00	0.01	0.00	0.01	0.00
Fe	0.11	0.00	0.00	0.00	0.01	0.01	0.00	0.00	0.1	0.01	0.01	0.05	0.11	0.16	0.00	0.06	0.01
E %	−0.4	−2.29	−0.61	−3.02	1.85	2.04	0.4	−2.64	−1.45	−2.77	1.44	−4.03	−5.23	5.96	−6.43	1.3	3.86

terlayered clay corrensite, probably developed in response to the thermal pulse, with a maximum temperature (probably close to 250°C) in the zone of wairakite.

Relation with pore-water profiles

The abundant zeolites in sediments from these reactive zones would explain the interstitial water composition profiles found in this forearc site (Figure 5). The uptake of water by highly hydrated neoformed silicates results in the high chlorinity of interstitial waters. In addition, the sodium concentration reaches a minimum value of 347 mM/liter at 257.4 mbsf (Blanc 1992). This corresponds to the depth where the amount of zeolite doubles. The decrease in Na-concentration of the interstitial water can be explained by the formation of abundant analcime. Such relations between the formation of secondary minerals from volcanic sediments and unusual interstitial water chemistry agree with observations made during the Leg 126 at Izu-Bonin forearc (Egeberg *et al* 1990, Egeberg 1992, Tazaki and Fyfe 1992).

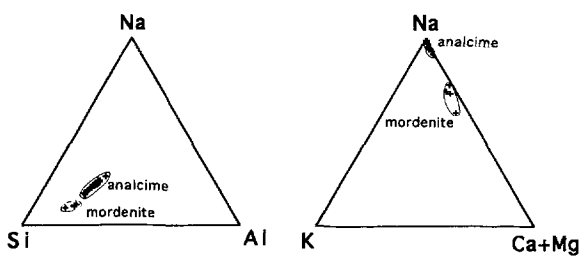

Figure 4. a. Distribution of major cations in atomic percent of representative analcime and mordenite from Hole 841. b. Distribution of exchangeable cations in atomic percent of representative analcime and mordenite from Hole 841.

Table 3d. Microprobe analyses (weight %) and structural formula (atomic coefficient) of mordenite from Hole 841, calculated on the basis of 96 oxygens, Core 135 841B 15R1 and 135 841B 29R1.

	15R1 ME2	15R1 ME4	15R1 ME5	29R1 DP25
SiO_2	71.94	73.54	74.09	78.69
Al_2O_3	15.72	16.67	15.97	12.94
MgO	0.76	0.39	0.00	0.00
CaO	4.00	2.9	3.62	2.85
Na_2O	5.07	5.93	5.5	5.1
K_2O	0.73	0.57	0.4	0.1
Fe_2O_3	1.78	0.00	0.42	0.32
Si	37.44	37.88	38.17	40.04
Al	9.64	10.12	9.7	7.76
Mg	0.59	0.3	0.00	0.00
Ca	2.23	1.6	2.00	1.55
Na	5.12	5.92	5.49	5.03
K	0.48	0.37	0.26	0.07
Fe	0.7	0.00	0.16	0.12
E %	−8.03	0.23	1.16	−3.88

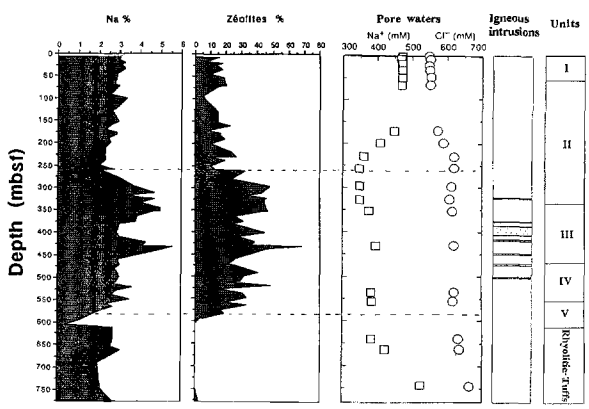

Figure 5. Comparison between the Na and zeolites content of the Hole 841 and the concentration with depth of Na^+ and Cl^- dissolved in the interstitial water.

https://doi.org/10.1346/CCMN.1995.0430111 Published online by Cambridge University Press

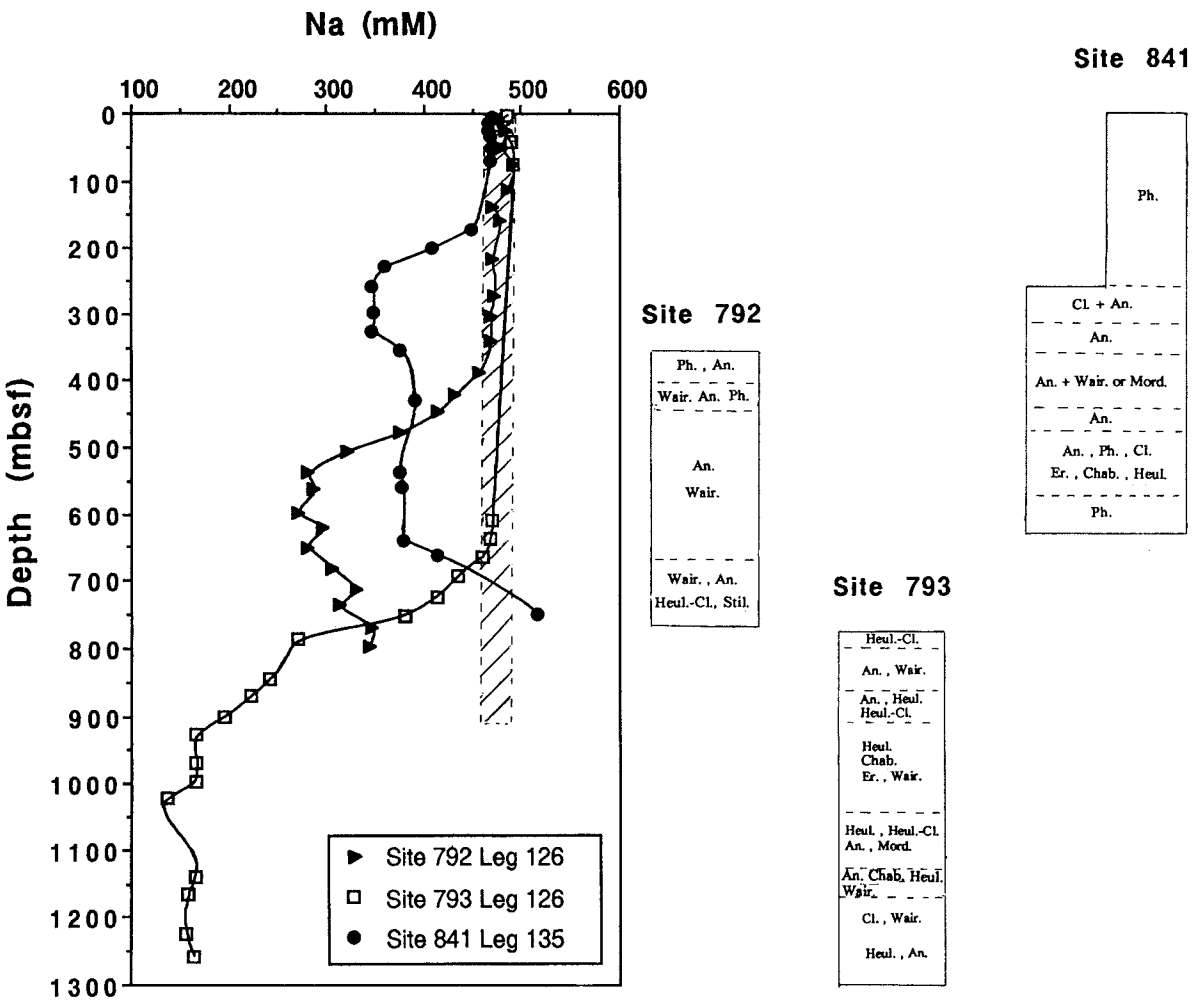

Figure 6. Unusual Na pore-water profiles, and zeolite distributions for Sites 792 and 793 from Leg 126, and Site 841 from Leg 135. Shaded zone represents the interval of Na-pore-water values sampled from the other Sites of Leg 126 and 135 (SW Pacific). An. = Analcime, Cl. = Clinoptilolite, Ph. = Phillipsite, Wair. = Wairakite, Er. = Erionite, Chab. = Chabazite, Mord. = Mordenite, Heul.-Cl = Heulandite-Clinoptilolite, Stil. = Stilbite.

Comparison with other SW Pacific sites

Profiles of interstitial water Na concentration vs. depth have been reported for all the SW Pacific sites of Leg 126 (Izu-Bonin) and Leg 135 (Lau and Tonga regions) (Figure 6). Most of the sites show normal Na pore-water values, which vary from 464 mM/liter to 493 mM/liter for Leg 126 sites (Egeberg 1992) and from 464 mM/liter to 489 mM/liter for Leg 135 Sites (Blanc *et al* 1994), with the exception of the following three sites: Hole 841 from the Tonga Trench margin (this paper), and Holes 792 and 793 from the Izu-Bonin Forearc (Egeberg 1992). The minimum pore-water Na-values reached were 270 mM/liter at 599.05 mbsf for Hole 792, 136 mM/liter at 1022.99 mbsf for Hole 793 and 347 mM/liter at 257.4 mbsf and 325.9 mbsf. The zones of zeolite occurrence for these Holes are given in Figure 6.

The compilation of data from different sources (Taylor *et al* 1990, Tazaki and Fyfe 1992, Marsaglia and Tazaki 1992) gives a schematic zeolite distribution profile with depth for Holes 792 and 793 in relation to pore-water chemical profiles (Figure 6). For Holes 792 and 793, the zones of Na-depleted pore-water correlate with the zones of zeolite occurrence, and the abundant formation of zeolite in highly altered tuff zones seems to explain the unusual pore-water profiles.

Samples from Sites 792 and 793 from the Izu-Bonin Forearc contain a wide variety of zeolite species, which show a great similarity with Hole 841 zeolites. Zeolite minerals identified include analcime, phillipsite, wairakite, heulandite and clinoptilolite for Hole 792 (Tazaki and Fyfe 1992). Analcime, mordenite, natrolite, heulandite, wairakite, chabazite, erionite, and phillipsite constitute the zeolite assemblage of Hole 793 (Mar-

saglia and Tazaki 1992). All the zeolite species found in Hole 841 deep sea sediments were also detected in Hole 793, including mordenite and erionite, which are rare in deep sea sediments. Secondary minerals such as analcime and clinoptilolite throughout the entire reactive zone probably constitute the major sink for Na from pore-water.

The original sediment grain size might play the most important role in controlling diagenetic reactions, as in the Izu-Bonin Forearc System. In the fine grained Miocene section of Holes 792 and 793, porosity averages 20% whereas in the vitric and pebbly sandstones of late Oligocene, it averages 50% (Taylor *et al* 1990). Oligocene volcaniclastic sandstones of the Izu-Bonin Forearc seem to have acted as redistributing conduits for fluids warmed by the post-Miocene intrusions. Warm water associated with intrusion may accelerate or intensify diagenetic reactions (Boles 1977). When these rising hot solutions encountered the finer grained, less permeable Miocene sections, they may have spread out laterally below this permeability barrier. This could explain the apparent higher degree of alteration in the more proximal site(s) to the intrusion(s) (e.g., Hole 793) (Marsaglia and Tazaki 1992).

A great difference between sites from Izu Bonin and from the Tonga Trench margin seems to be the role played by the sediment grain size in the control of diagenetic reactions. Its role appears clearly effective in Sites 792 and 793 from Izu-Bonin, where the variation of grain size is large, which is not the case in the sediment column of Hole 841 from the Tonga Trench margin (Parson *et al* 1992). In Hole 841, the abundance of zeolites in the lower part of Unit III and consequently the unusual pore-water values seem to be more closely associated with intrusions of igneous material into the sedimentary column than with the sediment composition. Although conventional contact metamorphic effects are usually restricted to within a few meters of an intrusive body, oxygen isotope studies suggest that intrusions are capable of heating porous and permeable country rocks to temperatures greater than 100°C at distances of at least three stock diameters from the intrusions (Taylor 1971). Thus, in areas where intercalated lavas and intrusive rocks are present, such as the Tonga Forearc Hole where nine igneous units were observed, zeolitization may have been influenced by the emplacement of these igneous rocks. Fluid flow induced by the intrusion of sills and dykes probably acts as a mechanism to transport heat in the sedimentary series. Veins of analcime/mordenite testified this assumption.

CONCLUSION

Mineralogical study of sediments from Hole 841 situated on the upper Tonga Trench slope show the importance of secondary mineral crystallization. Zeolites constitute the major authigenic minerals, and the zeolite distribution can be summarized from the top to the bottom of the sedimentary column by the sequence: (I) phillipsite, (II) clinoptilolite + analcime, (III) analcime (alone or occasionally with either wairakite or mordenite), (IV) analcime, phillipsite, clinoptilolite, erionite, chabazite, heulandite, (V) phillipsite.

This zeolite zonation in Hole 841 should be attributed to the superposition of two phenomena: At first, simple burial diagenesis with the formation of phillipsite and clinoptilolite, and secondly, a development of zeolites such as analcime, mordenite and wairakite, in response to heat flow resulting from the emplacement of intrusive basaltic andesite into the sedimentary column. Analcime, the most abundant zeolite mineral of the "baked" zone presents an average composition close to $Si_{33.5}Al_{14.5}Na_{14.5}Ca_{0.1}O_{96}.16H_2O$. The formation of abundant analcime in response to the thermal pulse may explain the unusual pore-water composition of this Tonga Trench margin Site. The planned future work consists of an oxygen isotope analysis of the clays and zeolites, in order to define the precise temperature of cristallization of the secondary minerals with the aim of constraining the diagenetic processes of the sedimentary pile.

REFERENCES

Bailey, S. W. 1982. Nomenclature for regular interstratification. *Clay Miner.* **17**: 243–248.

Bargar, K. E., M. H. Beeson, and T. E. C. Keith. 1981. Zeolites in Yellowstone National Park. *Miner. Record.* **12**: 29–38.

Barth-Wirsching, U., and H. Höller. 1989. Experimental studies on zeolite formation conditions. *Eur. J. Mineral.* **1**: 489–506.

Blanc, G. 1992. Interstitial water chemistry, Leg 135 Lau Basin and Tonga Ridge. In *Proceeding of the Ocean Drilling Program, Initial Report, Vol. 135.* College Station, Texas.

Blanc, G. 1994. Geochemical studies on selected sediment samples from the back-arc Lau basin, Leg 135 ODP. *Proceeding of the Ocean Drilling Program, Scientific Results* **135**: 689–708.

Blanc, G., P. Stille, and F. Vitali. 1994. Hydrogeochemistry in the Back-arc Lau Basin, ODP Leg 135. *Proceeding of the Ocean Drilling Program, Scientific Results* **135**: 677–688.

Boles, J. R. 1972. Composition, optical properties, cell dimensions and thermal stability of some heulandite group zeolites. *Am. Miner.* **57**: 1463–1493.

Boles, J. R. 1977. Zeolites in low-grade metamorphic grades. In *Mineralogy and Geology of Natural Zeolites.* F. A. Mumpton, ed. *Mineral. Soc. Am.* **4**: 103–135.

Boles, J. R., and W. S. Wise. 1978. Nature and origin of deep-sea clinoptilolite. In *Natural Zeolites. Occurrence, Properties, Use.* L. B. Sand and F. A. Mumpton, eds. Pergamon Press, 235–243.

Couture, R. A. 1977. Composition and origin of palygorskyte-rich and montmorillonite-rich zeolite-containing sediments from the Pacific ocean. *Chemical Geology* **19**: 113–130.

Desprairies, A., and C. Jehanno. 1983. Paragenèses minérales liées à des interactions basalte-sediment-eau de mer (Sites 465 et 456 des Legs 65 et 60 du D.S.D.P.). *Sci. Géol. Bull.* **36**: 93–110.

Egeberg, P. K. 1992. Thermodynamic aspects of Leg 126 interstitial waters. *Proceeding of the Ocean Drilling Program, Scientific Results, Vol. 126,* p. 519–529.

Egeberg, P. K., and the Leg 126 Shipboard Scientific Party. 1990. Unusual composition of pore waters found in the Izu-Bonin fore-arc sedimentary basin. *Nature* **344**: 215–218.

Giampaolo, C. 1986. Dehydration kinetics of thaumasite at ambient pressure. *N. Jb. Miner. Mh.* **3**: 126–134.

Gottardi, G., and E. Galli. 1985. *Natural Zeolites.* Berlin: Springer Verlag, 409 pp.

Hay, R. L. 1966. Zeolites and zeolitic reactions in sedimentary rocks. *Geological Society of America.* Special paper. 130 pp.

Hay, R. L. 1986. Geologic occurrence of zeolites and some associated minerals. In *New Developments in Zeolite Science Technology.* Y. Murakami, A. Ijima, and J. W. Ward, eds. *Proceeding of the 7th International Zeolite Conference* p. 35–40.

Hooton, D. H., and N. E. Giorgetta. 1977. Quantitative X-ray diffraction analysis by a direct calculation method. *X-Ray Spectrometry* **6**: 2–5.

Karpoff, A. M., C. France-Lanord, F. Lothe, and P. Karcher. 1992. Miocene tuff from Mariana basin, ODP Leg 129, Site 802. A first deep-sea occurrence of Thaumasite. *Proceeding of the Ocean Drilling Program, Scientific Results, Vol. 129,* p. 119–135.

Kastner, M., and S. A. Stonecipher. 1978. Zeolites in pelagic sediments of the Atlantic, Pacific, and Indian Oceans. In *Natural Zeolites. Occurrence, Properties, Use.* L. B. Sand and F. A. Mumpton, eds. Pergamon Press, 199–220.

Kristmannsdöttir, H., and J. Tomasson. 1978. Zeolite zones in geothermal areas Iceland. In *Natural Zeolites. Occurrence, Properties, Use.* L. B. Sand and F. A. Mumpton, eds., Pergamon Press, 277–284.

Kusakabe, H., H. Minato, M. Utada, and T. Yamanaka. 1981. Phase relations of clinoptilolite, mordenite, analcime and albite with increasing pH, sodium ion concentration and temperature. *University Tokyo Sci. Papers.* College of general education. Vol. 31, p. 39–59.

Liou, J. G. 1971. P-T stabilities of laumontite, wairakite, lawsonite, and related minerals in the system $CaAl_2Si_2O_8$-SiO_2-H_2O. *Journal of Petrology* **12**: 379–411.

Liou, J. G., C. De Capitani, and M. Frey. 1991. Zeolite equilibria in the system $CaAl_2Si_2O_8$-$NaAlSi_3O_8$-SiO_2-H_2O. *New Zealand Journal of Geology and Geophysics* **34**: 293–301.

Marsaglia, K. M., and K. Tazaki. 1992. Diagenetic trends in Leg 126 sandstones. *Proceeding of the Ocean Drilling Program, Scientific Results, Vol. 126,* p. 125–138.

Nakajima, W., and S. Ueda. 1990. Syntheses of natural zeolites. Syntheses of heulandite-clinoptilolite, analcime-wairakite, mordenite and ferrierite. *Nendo Kagaku.* **30**: 57–75 (in Japanese).

Parson, L., J. Hawkins, J. Allan, et al. 1992. *Proceeding of the Ocean Drilling Program, Initial Report, Vol. 135.* College Station, Texas, 677 pp.

Passaglia, E. 1970. The crystal chemistry of chabazites. *Amer. Miner.* **55**: 1278–1301.

Passaglia, E. 1975. The crystal chemistry of mordenites. *Contrib. Mineral. Petrol.* **50**: 65–77.

Passaglia, E., and G. Vezzalini. 1985. Crystal chemistry of diagenetic zeolites in volcanoclastic deposits of Italy. *Contrib. Mineral Petrol.* **85**: 190–198.

Passaglia, E., D. Pongiluppi, and R. Rinaldi. 1977. Merlinoite, a new mineral of the zeolite group. *N. Jb. Miner. Mh.* **8**: 355–364.

Schöps, D., and P. M. Herzig. 1994. Occurrence of Thaumasite in Lau Basin andesite of ODP Hole 841B, Leg 135. *Proceeding of the Ocean Drilling Program, Scientific Results* **135**: 689–708.

Seki, Y. 1973. Distribution and modes of occurrence of wairakites. *J. Geol. Soc. Jpn.* **79**: 521–527.

Seki, Y., H. Onuki, K. Okumura, and I. Takashima. 1969. Zeolite distribution in the Katayama geothermal area. *Jpn. J. Geol. Geogr.* **40**: 63–69.

Sheppard, R. A., A. Gude 3rd, and J. J. Fitzpatrick. 1988. Distribution, characterization, and genesis of mordenite in Miocene tuffs at Yucca Mountains, Nye County, Nevada. *U.S. Geol. Surv. Bull.* **1777**: 1–22.

Steiner, A. 1955. Wairakite, the calcium analogue of analcime, a new mineral. *Miner. Mag.* **30**: 691–698.

Stonecipher, S. A. 1976. Origin, distribution and diagenesis of phillipsite and clinoptilolite in deep-sea sediments. *Chemical Geology* **17**: 307–318.

Surdam, R. C. 1973. Low-grade metamorphism of tuffaceous rocks in the Karmutsen Group, Vancouver Island, British Columbia. *Geological Society of America Bulletin* **84**: 1911–1922.

Taylor, B., K. Fujoka, T. R. Janecek, et al. 1990. *Proceeding of the Ocean Drilling Program, Initial Report, Vol. 129.* College Station, Texas, 1002 pp.

Taylor, H. P. Jr. 1971. Oxygen isotope evidence for large-scale interaction between intrusions, Western Cascade Range, Oregon. *J. Geophys. Res.* **76**: 7855–7874.

Tazaki, K., and W. S. Fyfe. 1992. Diagenetic and hydrothermal mineral alteration observed in Izu-Bonin deep-sea sediments, Leg 126. *Proceedings of the Ocean Drilling Program, Scientific Results, Vol. 126,* p. 101–112.

Vitali, F., G. Blanc, P. Larqué, and J. Samuel. 1995. Geochemical trends of Site 840 from the Tonga Platform. A comparison with the others sites from Leg 135 ODP. *Oceanologica Acta* (in press).

(Received 15 September 1993; accepted 8 August 1994; Ms. 2416)